Experimental Hematology

Experimental Hematology 2019;69:27–36

Characterization of inv(3) cell line OCI-AML-20 with stroma-dependent CD34 expression

Genna M. Luciani[a,b,c], Lihua Xie[b,1], David Dilworth[a], Anne Tierens[d], Yoni Moskovitz[e], Alex Murison[b], Magdalena M. Szewczyk[a], Amanda Mitchell[b], Mathieu Lupien[b], Liran Shlush[e], John E. Dick[b], Cheryl H. Arrowsmith[a,b,c], Dalia Barsyte-Lovejoy[a], and Mark D. Minden[b,c]

[a]*Structural Genomics Consortium, University of Toronto, Toronto, Ontario, Canada;* [b]*Princess Margaret Cancer Centre, Toronto, Ontario, Canada;* [c]*Department of Medical Biophysics, University of Toronto, Ontario, Canada;* [d]*Toronto General Hospital, Laboratory Medicine Program, Toronto, Ontario, Canada;* [e]*Department of Immunology, Weizmann Institute of Science, Rehovot, Israel*

(Received 29 August 2018; revised 12 October 2018; accepted 15 October 2018)

Acute myeloid leukemia (AML) is a complex, heterogeneous disease with variable outcomes following curative intent chemotherapy. AML with inv(3) is a genetic subgroup characterized by a very low response rate to current induction type chemotherapy and thus has among the worst long-term survivorship of the AMLs. Here, we describe OCI-AML-20, a new AML cell line with inv(3) and deletion of chromosome 7; the latter is a common co-occurrence in inv(3) AML. In OCI-AML-20, CD34 expression is maintained and required for repopulation in vitro and in vivo. CD34 expression in OCI-AML-20 shows dependence on the co-culture with stromal cells. Transcriptome analysis indicates that the OCI-AML-20 clusters with other AML patient data sets that have poor prognosis, as well as other AML cell lines, including another inv(3) line, MUTZ-3. OCI-AML-20 is a new cell line resource for studying the biology of inv(3) AML that can be used to identify potential therapies for this poor outcome disease. © 2018 Published by Elsevier Inc. on behalf of ISEH – Society for Hematology and Stem Cells.

Acute myeloid leukemia (AML) is a heterogeneous disorder characterized by the abnormal proliferation and differentiation of hematopoietic stem cells. Patients diagnosed with AML often have a poor prognosis, with long-term survival being affected by subtype of disease, therapy given, and ability to tolerate treatment [1]. An important classifier of the disease that can predict response to therapy and outcome is the presence of recurrent cytogenetic abnormalities. Patients with recurrent 3q mutations such as inv(3)(q21q26.2) or t(3;3)(q21;q26.2) represent a subgroup of AML with a very poor prognosis due to the high rates of resistance to current chemotherapy regimens [2]. The inversion of the chromosome causes the overexpression of the proto-oncogene ectopic viral integration 1 (EVI1) [3–5]. The inversion occurs in approximately 1–2% of AML cases; an additional 11% of cases of AML have overexpression of EVI1 through different mechanisms and these patients have similarly poor outcome [6].

AML with inv(3) is frequently found to co-occur with other recurrent chromosome abnormalities such as t(9;21) or deletion/loss of chromosome 7 [2]. Two existing cell lines with inv(3) that have been used to study inv(3) AML are UCSD-AML1 and MUTZ-3 [7,8]. Both of these cell lines have very complex karyotypes [UCSD-AML1 10% polyploidy; 45(42–45)<2n>XX,-7, t(3;3)(q21;q26), t(12;22)(p13;q12), t(3;3) and t(12;22) and MUTZ-3 near-diploid karyotype with 6% tetraploidy - 46(44-48)<2n>XY, t(1;3)(q43;q13)inv(3)(q21q26), t(2;7)(q36;q36)inv(7)(p15q36),t(12;22)(p13;q12)], which may render it difficult to study the pathophysiologic mechanisms attributed to the overexpression of EVI-1.

Within the patient, AML cells reside in a complex microenvironment that includes bone marrow stroma cells and endothelial cells among many cell types. Since the long-term culture for normal hematopoietic cells, first described by Dexter et al. [9], there have been numerous studies employing stroma cell based microenvironment as a surrogate for the bone marrow

GML and LX contributed equally to this work.

Offprint requests to: Dr. Mark D. Minden, Department of Oncology/Hematology, Princess Margaret Hospital, 610 University Ave., Room 9-113, Toronto, Ontario, M5G 2M9 Canada; E-mail: mark.minden@uhn.ca

[1]LX's present address: Department of Hematology, Huashan Hospital, Fudan University, Shanghai, China.

Supplementary material associated with this article can be found, in the online version, at doi:10.1016/j.exphem.2018.10.006.

0301-472X/
https://doi.org/10.1016/j.exphem.2018.10.006

cell niche to study the molecular cross-talk, stem cell maintenance, and therapeutic resistance [10–14]. In this study, we established and characterized a new cell line, OCI-AML-20, which has inv(3) and loss of chromosome 7. The OCI-AML-20 cell line was established using the mesenchymal stem cell-like OP9 stroma cells [15] and the expression of the stem cell marker CD34 in OCI-AML-20 is dependent on co-culture with stroma. We show that CD34 expression correlates with the clonogenic growth and engraftment of OCI-AML-20 cells. These cells represent a novel, well-characterized system with which to study inv(3) AML, the dynamics and drivers of CD34 expression, and leukemia cell niche-type interactions with stroma cells and to identify potential therapies for this poor prognosis form of AML.

Methods

Patient history

A peripheral blood sample of a 34-year-old male patient with chemoresistant/persistent AML M4 was obtained following informed consent in accordance with the procedures prescribed by the Research Ethics Board of the University Health Network approval (REB #01-0573). The patient first presented in July 2007 and the sample from which the cell line was established was collected in June 2008. Before collection, the patient had been treated with the following chemotherapeutic agents: hydroxyurea, daunorubicin, and cytarabine (3+7), mitoxantrone and etoposide (NOVE), cyclophosphamide, and decitabine; at no time did the patient achieve remission. At presentation, the patient had the following peripheral blood cell counts: hemoglobin 116 g/L, platelets 147×10^9/L, white blood cells 143×10^9/L, and neutrophils 11.4×10^9/L. At the time of collection, the peripheral blood counts were: hemoglobin 77 g/L, platelets 16×10^9/L, white blood cells 206×10^9/L, neutrophils 16×10^9/L, and blasts 150×10^9/L. Peripheral blood mononuclear cells were separated by Ficoll-Hypaque centrifugation and subsequent storage at −150°C in 10% dimethylsulfoxide, 40% fetal calf serum, and alpha minimal essential medium (αMEM). Flow cytometry analysis of this sample confirmed the myeloid lineage of the leukemic cells with positivity for CD2, CD4, CD7, CD11b, CD13, CD33, and CD34; the sample was negative for cytoplasmic myeloperoxidase (Supplementary Table E1, online only, available at www.exphem.org). G-banding revealed an abnormal male karyotype 45,XY,inv(3)(q21q26.2),-7 in all 20 studied metaphases.

Establishment of cell line

Cryopreserved mononuclear cells were thawed, washed, and injected intrafemorally into nonobese diabetic/severe combined immune deficient mice as described previously [16]. Engrafted cells were characterized by the expression of human CD45 in the mouse bone marrow after 8–10 weeks. Cells recovered from mouse bone marrow were isolated and frozen viably as above and eventually used to establish the cell line. Following rapid thawing and washing, cells were grown in six different conditions (Supplementary Table E2, online only, available at www.exphem.org) in six-well plates previously seeded with OP9 stroma that had reached confluency. OP9 stroma (ATTC) was cultured in α-MEM media with GlutaMAX (Invitrogen) containing 20% fetal bovine serum (FBS) (Wisent), 55 μmol/L β-mercaptoethanol (Invitrogen) and 100U/100 μg/mL penicillin/streptomycin (Invitrogen). Immunophenotype was followed weekly. Media containing granulocyte-macrophage colony-stimulating factor (GM-CSF) was the most effective at maintaining the CD34 population of cells. MS5 stroma were also used to culture the cells using the same medium as OP9 but with 10% FBS added.

Flow cytometry and immunophenotypic profile

Cells were analyzed on a LSR-Fortessa X-20 machine using FACSDiva Software (version 8.0.1; BD Biosciences). The following antihuman antibodies were used at 1 μL for 1×10^5 cells: CD45-FITC (clone: HI30), CD-34-APC (clone: 581), and CD38-PE-Cy7 (clone: HB7/HIT2), all from BD Biosciences, and 7-amino-actinomycin D viability dye from Life Technologies. List mode files were analyzed using FlowJo (version 10).

In addition, the cells were further characterized using a comprehensive antibody panel employed at the Department of Hematopathology for the diagnosis of acute leukemia. This comprises four 10-color antibody combinations aimed at identifying the differentiation and maturation stages of the hematopoietic cell lineages and abnormal antigen expression (Supplementary Table E3, online only, available at www.exphem.org). The cells were washed and resuspended in phosphate-buffered saline (PBS) at 1×10^6 cells/mL. A 100 μL cell suspension was incubated with the respective antibody cocktails for 15 minutes in the dark at room temperature. Following incubation, cells were washed and resuspended in IOtest 3 Fixative (Beckman Coulter) and PBS. Staining for intracellular markers was performed using the IntraPrep kit (Immunotech) according to the manufacturer's instructions. Information for at least 1×10^5 cells was acquired on a Navios flow cytometer (Beckman Coulter) and analysis was done using the Infinicyt software version 1.7 (Cytognos).

Cell sorting was performed using cells collected in PBS with 2% FBS and stained for 10 minutes at room temperature with antibodies against human CD34-PE (clone: AC136; 1:41) and CD38-VioBright FITC (clone: REA671; 1:21) (Miltenyi Biotec), along with 0.2 μmol/L Sytox Blue (Life Technologies) viability dye. Sorting was performed using an AriaII-SC BRV at the SickKids University Health Network flow cytometry facility. Follow-up analysis of the sorted cultures was performed with the same antibodies using the MACSQuant VYB flow cytometer (Miltenyi Biotec) and analyzed with FlowLogic software.

Limiting dilution assays

Limiting dilution assays (LDAs) were performed in 96-well plates (Eppendorf) that were seeded with 5000 OP9 or MS5 cells the day before sorting. Unsorted and sorted cell populations were plated at 1, 10, 100, or 1000 cells per well on OP9 stroma. Wells with robust OCI-AML-20 cell growth

were scored 2–4 weeks later depending on cell density. Results were analyzed using ELDA: Extreme Limiting Dilution Analysis software [17].

Cytogenetics and short tandem repeat analysis

To confirm that the identity of OCI-AML-20 matched the original patient, short tandem repeat (STR) analysis on isolated genomic DNA (Invitrogen kit) and cytogenetics of the cell line were performed by The Centre for Applied Genomics; The Hospital for Sick Children, Toronto, Canada; and the Cytogenetics laboratory of University Health Network.

RNA sequencing

RNA was collected using TRIzol (Invitrogen) extraction. RNA concentration and quality was assessed using a Bioanalyzer (Agilent Technologies). Sample libraries were prepared using the Illumina TruSeq Stranded mRNA sample preparation kit. Sequencing was performed using Illumina NextSeq500 using 75-cycle paired-end protocol and multiplexing at the Princess Margaret Genomics Centre.

Western blot

Cell lysate preparation and Western blots were as described previously [18]. Blots were incubated overnight at 4°C with the antibodies for EVI1 (1:1000, Abcam #ab124934) and actin (1:3000, Abcam #3280). Secondary antibodies were: goat anti-rabbit IgG (IRDye 800-conjugated, LiCor #926-32211) and donkey anti-mouse IgG (IRDye 680-conjugated, LiCor #926-68072) antibodies (1:5000) in Odyssey blocking buffer (LiCor). The signal was read on an Odyssey scanner (LiCor) at 800 and 700 nm.

Green fluorescent protein/mCherry labeling of OCI-AML-20 and OP9 and suspension/adherent fraction assays

Lentivirus vector based on the pRRL vectors made by the Naldini laboratory (Addgene #12252) that was modified to express green fluorescent protein (GFP) or mCherry from the EF1 promoter was packaged by standard methods. OCI-AML-20 cells were transduced with pRRL- EF1-GFP and sorted as above. A similar procedure was used to obtain the mCherry-labeled OP9 using pRRL-EF1-mCherry. For the suspension fraction isolation, the cells were gently removed without disturbing the adherent layer and the remaining adherent cells were washed three times with PBS. The remaining adherent cells were trypsinized, counted, and transferred at different densities to a 96-well plate with OP9 cells. GFP and mCherry imaging was done using the IncuCyte ZOOM live-cell imaging device (Essen Bioscience) and analyzed with IncuCyte ZOOM software.

RNA-sequencing data processing and clustering analysis

RNA-sequencing (RNA-Seq) reads were aligned to the GRCh38 reference genome using a two-pass method with STAR 2 [19] (2.5.3a) following methods outlined by the Internal Cancer Genome Consortium. After alignment, reads were quality filtered using SAMtools [20] (version 1.3.1) and mapped reads enumerated using HT-Seq count [21] (version 0.9.1) with a GENCODE version 22 annotation file. For clustering analysis, TCGA-LAML gene level expression counts, as well as mutational and clinical data, were retrieved from The National Cancer Institute Genomic Data Commons using the R/Bioconductor package TCGAbiolinks [22] (version 2.7.9). The clustering analysis and heat map visualization were also generated using the TCGAbiolinks package, which implements features from the ComplexHeatmap [23] (version 1.14.0) and ConsensusClusterPlus [24] (version 1.40.0) packages. Additionally, MECOM FPKM expression values displayed in the clustering analysis were derived using DESeq2 [25] (version 1.16.1). For visualization of the MECOM locus, aligned read files were converted to bigWig format using deepTools [26] (version 2.5.1) and viewed on the UCSC Genome Browser. RNAseq data are available at the Gene Expression Omnibus website under accession number GSE120834.

Mutational analysis

The molecular inversion probe (MIP) capture protocol was adopted and modified from Hiatt et al. [27] and we designed an MIP probe set [28]. PCR primers, sequencing primers, and the MIP backbone were as described by Hiatt et al. [27]. For the probe hybridization step, 200 ng of template DNA was mixed with a MIP pool at a final concentration of 50 pmol per probe and in 1 × Ampligase buffer (Epicentre). This mixture was incubated in a thermal cycler at 98°C for 3 minutes, followed by a gradual thermal reduction to 85°C for 30 minutes and 60°C for 60 minutes. Subsequently, the reaction was incubated at 56°C for 36 hours. A gap-filling and ligation step were performed by mixing the 10 μL of the hybridization product with deoxynucleotide triphosphates (final concentration of 15 μmol/L), betaine (0.375 μmol/L), NAD^+ (1 mmol/L), ampligase buffer 0.5 ×, 1 μL of ampligase (0.25 U, Epicentre) and 1.6 μL of Phusion HF (0.16 U, New England Biolabs) in 20 μL. The mixture was incubated at 56°C for 60 minutes, followed by 72°C for 20 minutes. Enzymatic digestion of uncircularized probes and DNA was performed by adding 1 μL of Exonuclease I (20,000 units/mL, New England Biolabs) and 1 μL of Exonuclease III (100,000 units/mL, New England Biolabs), followed by incubation at 37°C for 2 hours and heat inactivation at 80°C for 20 minutes. To generate a final Illumina sequencing library, the final product (22 μL) was mixed with polymerase chain reaction (PCR) primers targeting the MIP backbone (0.5 μmol/L final concentration) with a different index sequence per sample and iProof HF Master Mix 1 × (Bio-Rad) at a final volume of 50 μL. PCR was performed by initial denaturation at 98°C for 30 sec and 26 cycles of 98°C for 7 sec, 55°C for 20 sec, and 72°C for 6 sec. A final extension was performed at 72°C for 7 minutes. Samples were pooled and purified using the Blue Pippin 2% cassette and sequenced in a NextSeq 500 in a 150 paired-end run. For variant calling, MIP ligation and extension arms were trimmed using cutAdapt directly from FATSQ files. Trimmed FASTQ files were aligned to human genome build 19 using the BWA-MEM protocol. Bam files were sorted by SAM tools followed by indel realignment. Realigned BAM files were converted to FREQ files as described in the IDES pipeline [29] and variants were annotated by Annovar [30]. Somatic mutations were called when coverage was >100 variant allele frequency >0.3 and <0.6 and the Kaviar allele frequency was <0.001 (Supplementary Table E4, online only, available at www.exphem.org). Indels were called using Mutect2 with the same criteria for somatic variants.

Results

Establishment of OCI-AML-20

Cryopreserved cells from the xenograft were plated on OP9 cells as a co-culture in six different media (Supplementary Table E2, online only, available at www.exphem.org). At the initial thaw, the majority of hCD45$^+$ cells were CD34$^+$ (Figures 1A and 1B). Over 4 weeks, media 3 (containing stem cell factor [SCF], GM-CSF, FMS-like tyrosine kinase 3 ligand (FLT3L), thrombopoietin [THPO], and interleukin-3 [IL-3]) consistently maintained the proliferation and phenotype of the cells (Figures 1A and 1B). Subsequently, we determined that OCI-AML-20 proliferation and CD34 expression were maintained over an extended period of time on OP9 stroma and GM-CSF as the only added cytokine (Supplementary Figure E1, online only, available at www.exphem.org).

Cell surface markers of OCI-AML-20

OCI-AML-20 cells displayed typical blast morphology with large nuclei and no granulation (Figure 1C). In addition, a few maturing granulocytes and monocytes were present (Figure 2A and Supplementary Figure E2, online only, available at www.exphem.org). The OCI-AML-20 cells were mostly CD45 dim and could be separated into CD34 bright and CD34 dim positive cells (Figure 2B and Supplementary Figure E2, online only, available at www.exphem.org). The immunophenotype of the two CD34 subsets is summarized in Figure 2C. Interestingly, the CD34$^+$ cells were CD117 (c-Kit) high but CD123 (IL-3 receptor) low and also displayed a CD7 subpopulation.

CD34 expression and proliferation dependence on OP9 stroma cells

To determine whether OCI-AML-20 cells are dependent on the stroma, we cultured cells in the presence or absence of stroma. Cells were grown either in suspension or in co-culture with OP9 stroma cells or with another commonly used stromal line, MS5. OCI-AML-20 cells grown in suspension culture with GM-CSF 20 ng/mL for 2 weeks resulted in loss of the majority of CD34 expression and poor clonogenic growth in LDAs (Figure 3A and Supplementary Table E5, online only, available at www.exphem.org). Interestingly, it was possible to enhance the proportion of CD34$^+$ cells in OCI-AML-20 when the cells were transferred back

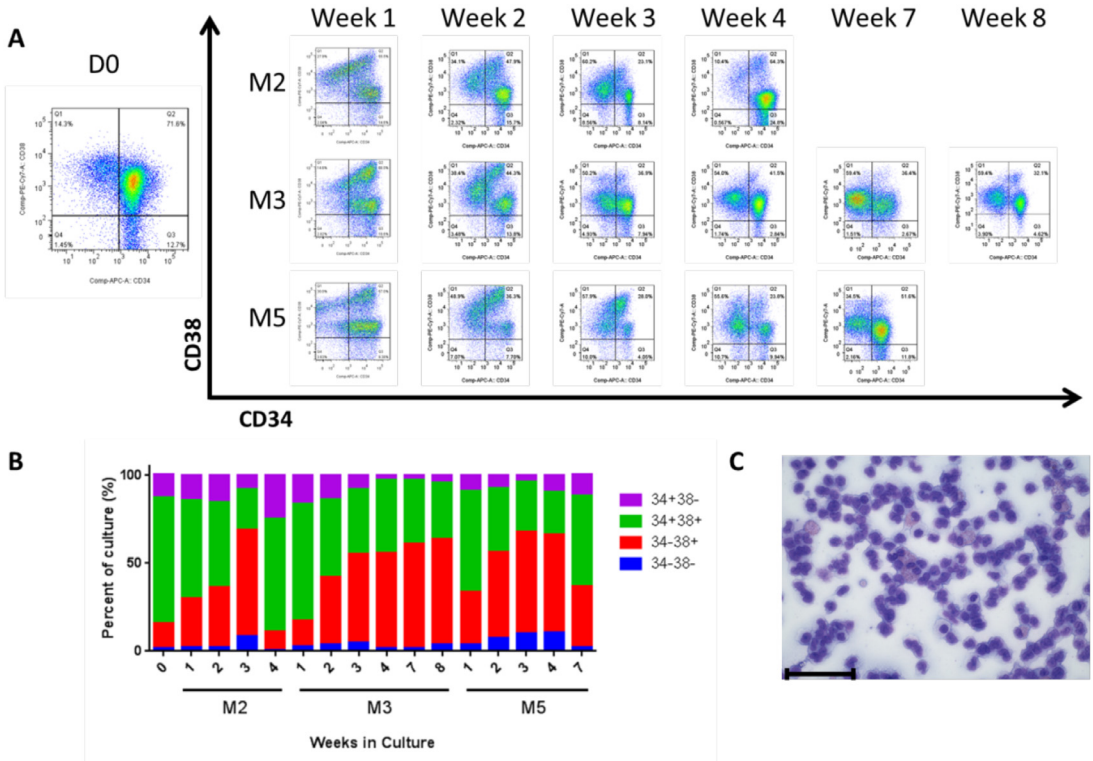

Figure 1. Establishment and morphology of cell line OCI-AML-20. **(A)** CD34 and CD38 were analyzed over weeks to determine an optimal condition for proliferation and maintenance of the stem cell marker CD34 on OCI-AML-20. M = media (see Supplementary Table E2, online only, available at www.exphem.org, for media composition); M2 = serum-free media with SCF, FLT3L, IL3, and G-CSF; M3 = media with SCF, FLT3L, IL3, GM-CSF, and THPO; M5 = media with IL3, G-CSF, and THPO. **(B)** Summary of CD34 and CD38 expression in different media after weeks in culture. **(C)** Cytospin image of OCI-AML-20. Scale bar indicates 100 μm.

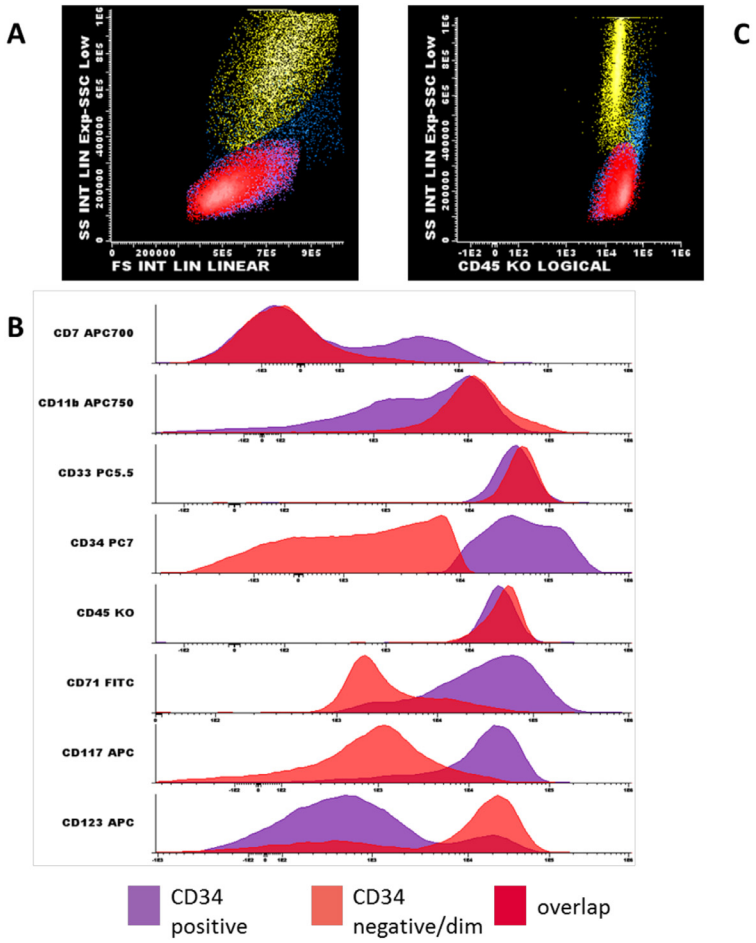

C

Antigens \ Subsets	CD34 bright positive subset	CD34 dim/negative
Lymphoid lineage antigens		
CD2	negative	negative
CD3	negative	negative
CD4	positive	positive
CD7	positive	negative
CD10	negative	negative
CD19	negative	negative
CD22	negative	negative
CD79a	negative	negative
CD56	positive	negative
Tdt	negative	negative
Myeloid antigens		
CD11b	subset positive	positive
CD11c	positive	positive
CD14	negative	negative
CD15	negative	negative
CD16	negative	negative
CD33	positive	positive
CD36	positive	negative
CD64	dim positive	subset positive
CD65	negative	negative
CD71	bright positive	dim positive
CD235a	negative	negative
MPO	negative	small subset positive
Progenitor/Precursor/Activation antigens		
CD34	bright positive	dim positive to negative
CD38	dim positive	subset bright positive
CD117	positive	negative
CD123	negative	positive
HLA-DR	positive	negative

Figure 2. Immunophenotypic profile of OCI-AML-20 culture. **(A)** Dot plots showing the light scatter characteristics and CD45 expression for the subsets in the cell culture. Red and violet dots represent CD34 bright positive and CD34 dim to negative cells, respectively, whereas the blue and yellow dots represent monocytes and granulocytes, respectively. **(B)** Respective histograms for the expression of CD45, CD34, CD117, CD33, CD7, CD11b, CD71, and CD123 by $CD34^+$ cells (purple), CD34 dim/negative (light red), or both CD34 subsets (red). X axis indicates the marker intensity and the Y axis represents a number of cells/events. **(C)** Summary of immunophenotype of OCI-AML-20. MPO = myeloperoxidase; Tdt = terminal deoxynucleotidyl transferase.

onto either stroma for 1 week with GM-CSF; this effect was more pronounced after 2 weeks of culture (Figures 3B and 3C).

To determine what population is responsible for establishing and maintaining the OCI-AML-20 line, cells were sorted into three groups: $CD34^+CD38^-$, $CD34^+CD38^+$, and $CD34^-$. $CD34^+$ cells showed robust proliferation after 1 and 2 weeks irrespective of CD38 expression in the presence of stroma and GM-CSF (Figure 3D). In contrast, $CD34^-$ cell proliferation was poor and the population was exhausted after 2 weeks on stroma with GM-CSF (Figure 3D and Supplementary Figure E3A, online only, available at www.exphem.org). LDAs on OP9 stroma further confirmed that CD34 expression correlates with the long-term growth potential of the cell line with an estimated stem cell frequency of approximately 1 in 2 cells for $CD34^+$ cells versus 1 in 15,405 for $CD34^-$ cells (Supplementary Figure E3B, online only, available at www.exphem.org). A similar reliance on CD34-expressing cells for cell line viability and expansion was noted for in vivo engraftment (Supplementary Table E6, online only, available at www.exphem.org).

OCI-AML-20 maintains a stable karyotype and EVI1 overexpression

We confirmed that OCI-AML-20 matched the original patient cells using STR (Supplementary Table E7, online only, available at www.exphem.org). The karyotype for OCI-AML-20 was determined to be 45,XY,inv(3)(q21q26.2),-7[5], which matches the presentation karyotype of 45,XY,inv(3)(q21q26.2),-7[20] (Figure 4A and Supplementary Figure E4, online only, available at www.exphem.org).

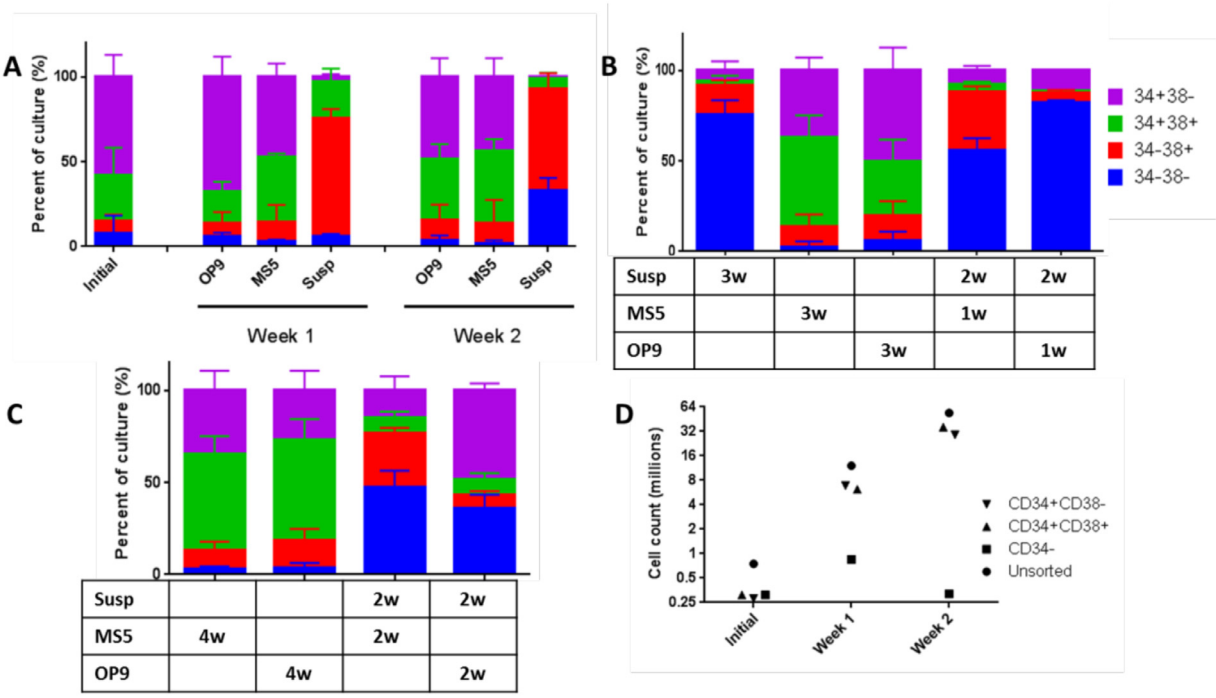

Figure 3. Persistence of CD34-expressing cells is dependent on the presence of stroma. In addition, the clonogenic cells of OCI-AML-20 reside in the $CD34^+$ subset of cells. **(A)** OCI-AML-20 CD34-expressing cells (purple and green bars) are maintained in the presence of either OP9 (mouse) or MS5 (mouse) stromal cells, but are decreased in the absence of stroma. Susp = suspension. **(B)** CD34 expression displays dependency on stroma in OCI-AML-20 cells. The cell population grown in suspension for 3 weeks loses CD34 expression but can regain expression seen on stroma if transferred back to stroma for 1 week (w) or **(C)** 2 weeks. **(D)** Sorted OCI-AML-20 of pure populations with CD34/CD38 expression was investigated for long-term repopulation capacity.

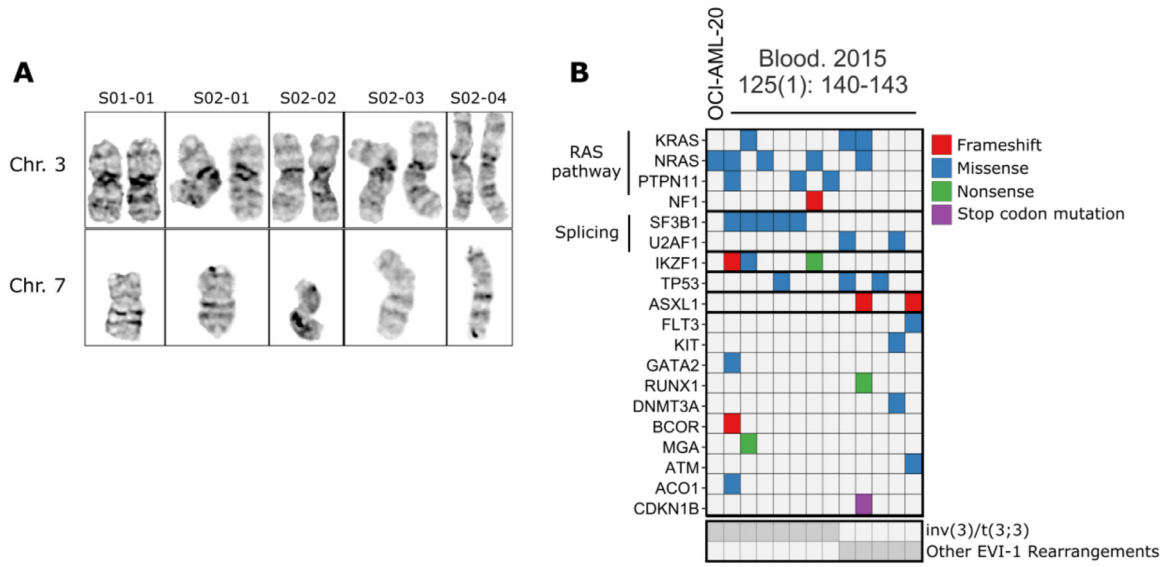

Figure 4. Karyotype and mutational profile of OCI-AML-20 cell line. **(A)** Metaphase spreads of chromosomes 3 and 7 from OCI-AML-20, in which a 45,XY,inv(3)(q21q26.2),-7 [5] karyotype is observed, corresponding with the patient karyotype at diagnosis. **(B)** Comparison of OCI-AML-20 mutational profile with EVI1-rearranged AML patient samples described previously [31].

Mutational profile of OCI-AML-20

To further characterize the genetic background of OCI-AML-20, we performed targeted DNA sequencing of genomic DNA of the original patient sample to identify genetic variants. In total, we observed three somatic mutations. The only coding region mutation was the recurrent NRAS (Q61K) with a variant allele frequency of 47.7% (Supplementary Table E4, online only,

available at www.exphem.org). The RAS/RTK signalling pathway is commonly activated in EVI1-rearranged AML (Figure 4B) [31]. No coding indels could be identified.

Transcriptome analysis

We next performed RNA-Seq analysis to compare the baseline transcriptome of OCI-AML-20 with existing publically available cell line and patient gene expression data. Visualization of the MECOM locus shows that the inv(3)(q21q26.2) rearrangement in OCI-AML-20 promotes overexpression of the *EVI1* transcript (Figure 5A). Additionally, by Western blotting, we observed elevated EVI1 protein levels with no detectable expression of amino-terminal epitopes present in MECOM, the carboxyl region of which contains EVI1 (Supplementary Figure E5, online only, available at www.exphem.org). To compare the transcriptional profile of OCI-AML-20 with established leukemia–lymphoma cell lines, we performed principle component analysis (PCA) with gene expression data available from the Cancer Cell Line Encyclopedia [32,33]. This analysis showed that OCI-AML-20 clusters with AML cell lines and is transcriptionally distinct from other types of leukemia and lymphoma cell lines (Supplementary Figure E6, online only, available at www.exphem.org). Focusing on only AML, PCA analysis grouped OCI-AML-20 in a distinct expression cluster that included MUTZ-3, another inv(3) cell line (Figure 5B). Hierarchical clustering analysis

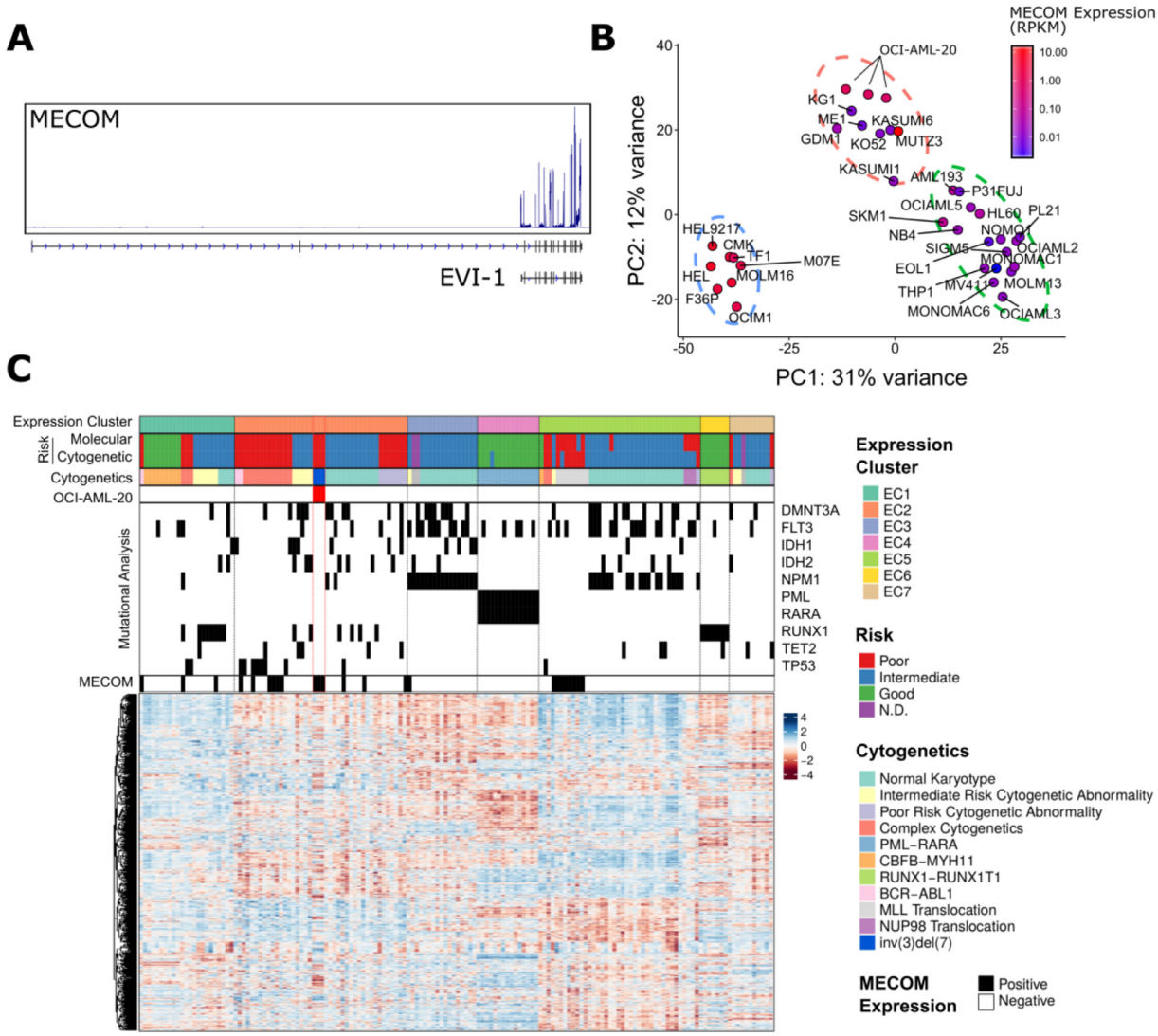

Figure 5. Transcriptomic analysis of OCI-AML-20. **(A)** Visualization of RNA-Seq gene expression data at the MECOM locus showing expression of the EVI-1 isoform. **(B)** PCA of OCI-AML-20 and AML cell line gene expression data obtained from the CCLE [32,33]. Data points are colored by MECOM expression level. **(C)** Clustering analysis of OCI-AML-20 RNA-Seq data with TCGA-LAML [34] patient gene expression annotated with clinical information, mutational data, and MECOM locus expression status. Three biological replicates of OCI-AML-20 are shown.

of OCI-AML-20 with the TCGA-LAML dataset [34] revealed that OCI-AML-20 shares a similar gene expression profile with intermediate- to high-risk patient populations and is seen in expression cluster 2 (EC2) (Figure 5C). Within EC2, we also observed enrichment of MECOM expression, which is also present in EC5 MLL translocation patient samples known to be positive for expression of MECOM [35]. Using this approach, we showed that common cytogenetic abnormalities group by expression cluster; for example, PML-RAR translocations found in acute promyelocytic leukemia cluster together in EC4 (Figure 5C). It should be noted that the dataset does not contain inv(3) patient samples.

OCI-AML-20 cell line subpopulations

On stroma cells, OCI-AML-20 exhibits a semi-adherent growth pattern without the classical cobblestone morphology [9]. To better visualize the interaction between OCI-AML-20 and stroma, we generated GFP-labeled OCI-AML-20 cells and mCherry-labeled OP9 cells. We observed that cells in suspension that are semi-adherent contained the proliferating/self-renewing fraction, whereas tightly adherent cells were unable to regenerate the cell line and are therefore most likely a terminally differentiated fraction (Figures 6A and 6B).

Discussion

Cell lines derived from AML patient cells are extensively used to identify therapeutic agents in vitro and in vivo. However, the majority of leukemia cell lines have complex cytogenetics and many of the existing lines are not representative of a recurring subset of AML patients [36]. In this report, we describe OCI-AML-20, a new EVI1-rearranged cell line that complements the previously described cell lines with inv(3) UCSD-AML1 and MUTZ-3 [7,8]. However, unlike the existing lines with complex karyotypes, the genetic makeup of OCI-AML-20 as determined to date includes a 46,XY,inv(3)(q21.3;q26.2),-7 and activating Q61K NRAS mutation. This constellation of abnormalities is not uncommon in primary AML patients [31,37].

The MECOM locus at 3q26.2 encodes for two transcripts and proteins. The full-length MECOM protein is 1239 amino acids, whereas the EVI1 protein is lacking the PR-SET domain at the N terminus and thus comprises only the carboxyl end of MECOM. In some AML cases, either through inv(3) rearrangement or a t (3;3) translocation, only the shorter EVI1 is made. AML cases with these chromosome changes typically do not achieve remission with current curative intent therapies; therefore, there are only rare patients with long-term survival. AML cases with inv(3) have high level expression of CD13, CD33, CD34, CD38, and CD117 (c-Kit) and variable expression of CD7, CD41, and CD61. Consistent with this, OCI-AML-20 has high levels of expression of CD34, CD38, CD33, CD117, and CD7 and the stem cell-associated $CD34^+$ subset of cells are positive for CD117 and CD7.

In initiating the cell line, we used a combination of OP9 stroma cells and a cytokine cocktail that contained SCF, GM-CSF, FLT3L, THPO, and IL-3. Once established, the cells required the continued presence of GM-CSF and stroma, the latter of which is a source of SCF. Grown under these conditions, we found that the cells continued to express the cell surface stem cell marker CD34 on a proportion of cells. With GM-CSF but no stroma, the proportion of $CD34^+$ cells declined and growth ceased; cells replated onto stroma with GM-CSF could recover growth and a $CD34^+$ population of cells. Using cell sorting and limiting dilution onto stroma with GM-CSF or injection into immune-deficient mice, we found that the cells able to grow and maintain the line were in the $CD34^+$ fraction; $CD34^-$ cells did not grow in mice or on stroma. Such a differentiation hierarchy is typical of human AML.

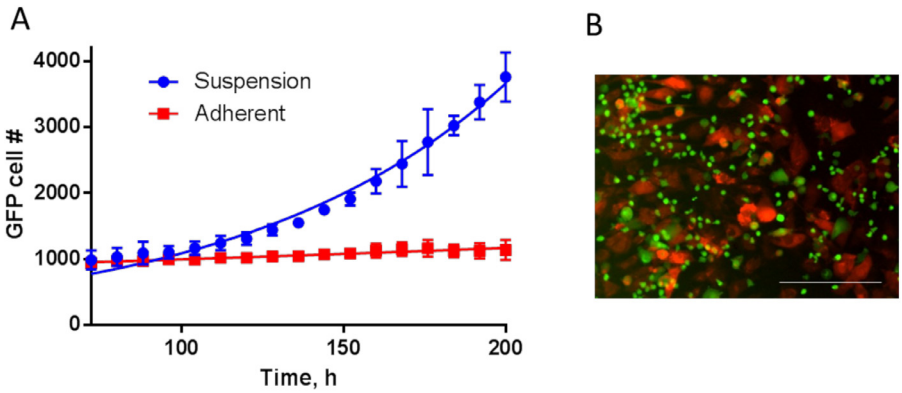

Figure 6. OCI-AML-20 GFP growth parameters. **(A)** Suspension and adherent fraction proliferation. Population doubling time 57 hours over the indicated period. **(B)** GFP-labeled OCI-AML-20 cells grown on mCherry-labeled OP9. Note larger adherent cells that were utilized in **(A)**. Variable mCherry signal results from individual OP9 cell bodies are shown. Scale bar indicates 300 μm.

The fact that such a hierarchy is preserved in OCI-AML-20, along with the continued dependence on stroma and growth factors, provides an opportunity to study the programs that are responsible for maintaining this structure. OCI-AML-20 will be available to the research community upon request and it is our expectation that the use of this cell line will help in identifying new approaches to treating a form of AML that has an unfortunately predictable mortality.

Acknowledgments

The authors thank Alma Seitova (Structural Genomics Consortium) and Dan Mamelak Custom Biologics (CB) for help with cytokines.

This work was supported by the Leukemia Lymphoma Society of Canada. The Structural Genomics Consortium is a registered charity (1097737) that receives funds from AbbVie; Bayer Pharma AG; Boehringer Ingelheim; Canada Foundation for Innovation; Eshelman Institute for Innovation; Genome Canada; Innovative Medicines Initiative (EU/EFPIA) (ULTRA-DD grant no. 115766); Janssen; Merck & Co.; Novartis Pharma AG; Ontario Ministry of Economic Development and Innovation; Pfizer; São Paulo Research Foundation-FAPESP; Takeda; and the Wellcome Trust.

References

1. Gregory TK, Wald D, Chen Y, Vermaat JM, Xiong Y, Tse W. Molecular prognostic markers for adult acute myeloid leukemia with normal cytogenetics. J Hematol Oncol. 2009;2:23.
2. Lugthart S, Gröschel S, Beverloo HB, et al. Clinical, molecular, and prognostic significance of WHO type inv(3)(q21q26.2)/t(3;3)(q21;q26.2) and various other 3q abnormalities in acute myeloid leukemia. J Clin Oncol. 2010;28:3890–3898.
3. Barjesteh van Waalwijk van Doorn-Khosrovani S, Erpelinck C, van Putten WL, et al. High EVI1 expression predicts poor survival in acute myeloid leukemia: a study of 319 de novo AML patients. Blood. 2003;101:837–845.
4. Glass C, Wilson M, Gonzalez R, Zhang Y, Perkins AS. The role of EVI1 in myeloid malignancies. Blood Cells Mol Dis. 2014;53:67–76.
5. Goyama S, Yamamoto G, Shimabe M, et al. Evi-1 is a critical regulator for hematopoietic stem cells and transformed leukemic cells. Cell Stem Cell. 2008;3:207–220.
6. Gröschel S, Lugthart S, Schlenk RF, et al. High EVI1 expression predicts outcome in younger adult patients with acute myeloid leukemia and is associated with distinct cytogenetic abnormalities. J Clin Oncol. 2010;28:2101–2107.
7. MacLeod RA, Hu ZB, Kaufmann M, Drexler HG. Cohabiting t(12;22) and inv(3) primary rearrangements in an acute myelomonocytic leukemia (FAB M4) cell line. Genes Chromosomes Cancer. 1996;16:144–148.
8. Oval J, Smedsrud M, Taetle R. Expression and regulation of the evi-1 gene in the human factor-dependent leukemia cell line, UCSD/AML1. Leukemia. 1992;6:446–451.
9. Dexter TM, Wright EG, Krizsa F, Lajtha LG. Regulation of haemopoietic stem cell proliferation in long term bone marrow cultures. Biomedicine. 1977;27:344–349.
10. Konopleva M, Konoplev S, Hu W, Zaritskey AY, Afanasiev BV, Andreeff M. Stromal cells prevent apoptosis of AML cells by up-regulation of anti-apoptotic proteins. Leukemia. 2002;16:1713–1724.
11. Coulombel L, Eaves AC, Eaves CJ. Enzymatic treatment of long-term human marrow cultures reveals the preferential location of primitive hemopoietic progenitors in the adherent layer. Blood. 1983;62:291–297.
12. Deneault E, Wilhelm BT, Bergeron A, Barabé F, Sauvageau G. Identification of non-cell-autonomous networks from engineered feeder cells that enhance murine hematopoietic stem cell activity. Exp Hematol. 2013;41:470–478.e4.
13. Garrido SM, Appelbaum FR, Willman CL, Banker DE. Acute myeloid leukemia cells are protected from spontaneous and drug-induced apoptosis by direct contact with a human bone marrow stromal cell line (HS-5). Exp Hematol. 2001;29:448–457.
14. Hartwell KA, Miller PG, Mukherjee S, et al. Niche-based screening identifies small-molecule inhibitors of leukemia stem cells. Nat Chem Biol. 2013;9:840–848.
15. Gao J, Yan XL, Li R, et al. Characterization of OP9 as authentic mesenchymal stem cell line. J Genet Genomics. 2010;37:475–482.
16. Mazurier F, Doedens M, Gan OI, Dick JE. Rapid myeloerythroid repopulation after intrafemoral transplantation of NOD-SCID mice reveals a new class of human stem cells. Nat Med. 2003;9:959–963.
17. Hu Y, Smyth GK. ELDA: extreme limiting dilution analysis for comparing depleted and enriched populations in stem cell and other assays. J Immunol Methods. 2009;347:70–78.
18. Eram MS, Shen Y, Szewczyk M, et al. A potent, selective, and cell-active inhibitor of human type i protein arginine methyltransferases. ACS Chem Biol. 2016;11:772–781.
19. Dobin A, Davis CA, Schlesinger F, et al. STAR: ultrafast universal RNA-seq aligner. Bioinformatics. 2013;29:15–21.
20. Li H, Handsaker B, Wysoker A, et al. The Sequence Alignment/Map format and SAMtools. Bioinformatics. 2009;25:2078–2079.
21. Anders S, Pyl PT, Huber W. HTSeq–a Python framework to work with high-throughput sequencing data. Bioinformatics. 2015;31:166–169.
22. Colaprico A, Silva TC, Olsen C, et al. TCGAbiolinks: an R/Bioconductor package for integrative analysis of TCGA data. Nucleic Acids Res. 2016;44:e71.
23. Gu Z, Eils R, Schlesner M. Complex heatmaps reveal patterns and correlations in multidimensional genomic data. Bioinformatics. 2016;32:2847–2849.
24. Wilkerson MD, Hayes DN. ConsensusClusterPlus: a class discovery tool with confidence assessments and item tracking. Bioinformatics. 2010;26:1572–1573.
25. Love MI, Huber W, Anders S. Moderated estimation of fold change and dispersion for RNA-seq data with DESeq2. Genome Biol. 2014;15:550.
26. Ramírez F, Ryan DP, Grüning B, et al. deepTools2: a next generation web server for deep-sequencing data analysis. Nucleic Acids Res. 2016;44:W160–W165.
27. Hiatt JB, Pritchard CC, Salipante SJ, O'Roak BJ, Shendure J. Single molecule molecular inversion probes for targeted, high-accuracy detection of low-frequency variation. Genome Res. 2013;23:843–854.
28. Shlush LI. Age-related clonal hematopoiesis. Blood. 2018;131:496–504.
29. Newman AM, Lovejoy AF, Klass DM, et al. Integrated digital error suppression for improved detection of circulating tumor DNA. Nat Biotechnol. 2016;34:547–555.
30. Yang H, Wang K. Genomic variant annotation and prioritization with ANNOVAR and wANNOVAR. Nat Protoc. 2015;10:1556–1566.
31. Lavallée VP, Gendron P, Lemieux S, D'Angelo G, Hébert J, Sauvageau G. EVI1-rearranged acute myeloid leukemias are characterized by distinct molecular alterations. Blood. 2015;125:140–143.

32. Barretina J, Caponigro G, Stransky N, et al. The Cancer Cell Line Encyclopedia enables predictive modelling of anticancer drug sensitivity. Nature. 2012;483:603–607.
33. Cancer Cell Line Encyclopedia Consortium; Genomics of Drug Sensitivity in Cancer Consortium. Pharmacogenomic agreement between two cancer cell line data sets. Nature. 2015;528:84–87.
34. Cancer Genome Atlas Research Network, Ley TJ, Miller C, Ding L, et al. Genomic and epigenomic landscapes of adult de novo acute myeloid leukemia. N Engl J Med. 2013;368:2059–2074.
35. Bindels EM, Havermans M, Lugthart S, et al. EVI1 is critical for the pathogenesis of a subset of MLL-AF9-rearranged AMLs. Blood. 2012;119:5838–5849.
36. Lübbert M, Koeffler HP. Myeloid cell lines: tools for studying differentiation of normal and abnormal hematopoietic cells. Blood Rev. 1988;2:121–133.
37. Gröschel S, Sanders MA, Hoogenboezem R, et al. Mutational spectrum of myeloid malignancies with inv(3)/t(3;3) reveals a predominant involvement of RAS/RTK signaling pathways. Blood. 2015;125:133–139.